Tetrahedron 69 (2013) 8186–8190

Contents lists available at SciVerse ScienceDirect

Tetrahedron

journal homepage: www.elsevier.com/locate/tet

Synthesis of elongated cavitands via click reactions and their use as chemosensors

Zsolt Csók[a,d,*], Tímea Kégl[a,d], Yin Li[b,d], Rita Skoda-Földes[c], László Kiss[b,d], Sándor Kunsági-Máté[b,d], Matthew H. Todd[e], László Kollár[a,d,*]

[a] Department of Inorganic Chemistry and MTA-PTE Research Group for Selective Chemical Synthesis, University of Pécs, H-7624 Pécs, P.O. Box 266, Hungary
[b] Department of General and Physical Chemistry, University of Pécs, Ifjúság 6., H-7624 Pécs, Hungary
[c] Department of Organic Chemistry, Institute of Chemistry, University of Pannonia, Egyetem 10., H-8200 Veszprém, Hungary
[d] János Szentágothai Research Center, Ifjúság 20., H-7624 Pécs, Hungary
[e] School of Chemistry, University of Sydney, NSW 2006, Australia

ARTICLE INFO

Article history:
Received 14 April 2013
Received in revised form 17 June 2013
Accepted 11 July 2013
Available online 18 July 2013

Keywords:
Cavitand
Azide–alkyne cycloaddition
Copper
Iron
Palladium

ABSTRACT

A very efficient modular reaction protocol was developed to attach various functionalities to a rigid cavitand scaffold. In this way, aryl, iodoaryl, benzyl, pyrrolidylmethyl groups, as well as a polyethylene-glycol chain were attached to the 'triazol-level' of the cavitand. The palladium-catalyzed ethynylation of the iodoarene moieties, followed by the copper(I)-catalyzed azide–alkyne cycloaddition produced novel cavitands with significantly elongated binding pockets. The dimensions of these molecules are calculated to be at least 9 Å×18 Å, which place them amongst the largest *unimolecular* hosts obtained by pure covalent synthesis. A cavitand-based click conjugate is used for selective complexation of Cu^{2+} and Fe^{3+}, providing significant fluorescent quenching.

1. Introduction

Cavitands are a class of molecular hosts containing sizeable internal cavities suitable for reversible molecular inclusion.[1] Cavitands and related cage-like structures show promise with potential applications as gas sensors, fluorescent probes, nanoreactors and drug delivery systems.[2,3] In our current research program, we aim to extend the inner cavity of such molecular containers through a modular strategy.[4,5] Click reactions, both minimizing the generation of hazardous substances and maximizing the reaction efficiency, are excellent representatives of the 'green chemistry' approach, an important contribution to sustainable development. The synthetic utility and simplicity of the very efficient copper(I)-catalyzed azide–alkyne cycloaddition (CuAAC),[6–8] coupled with a wide variety of readily available azide derivatives, opens up the avenue to the facile synthesis of highly extended macrocycles. The click coupling has recently been applied to cavitands for attaching guanosine[9] or uridine[10] moieties as well as macromolecular side chains[11] via triazole linkers, or alternatively, for covalently linking two macrocycle units.[12,13] Herein, we expand further the applicability of this versatile methodology by the synthesis of a novel series of elongated cavitands.

Click-derived triazoles have recently emerged as potential chemosensors due to their ability to bind both cations and anions. Sensitive reporting signals may arise from a binding event, a chemical reaction, a redox process or a conformational change.[14] Calixarenes are known to provide a convenient platform for positioning two[15–18] or four[19] triazole units in close proximity. These conjugates obtained by click chemistry were used to detect various metal ions including Hg^{2+}, Cu^{2+}, Cr^{3+}, Pb^{2+}, Zn^{2+} and Cd^{2+} through a photophysical change upon a binding event. The selectivity of the designed chemosensors greatly depended on the specific structural motifs that were incorporated into the macrocycle.

Here we report the first cavitand-based click conjugate that is used for selective complexation of Cu^{2+} and Fe^{3+}. These redox active metals undergo redox cycling reactions producing highly reactive radicals, which may eventually lead to oxidative stress in humans.[20] Therefore, it is very important to be able to monitor the presence of such metals. In contrast to the calixarene-based fluorescent probes that contained *pendant* functionalities for metal detection,[15–19] in our design the four triazole binding sites are attached on a more rigid cavitand framework, which

---

[*] Corresponding authors. E-mail addresses: zscsok@gamma.ttk.pte.hu (Z. Csók), kollar@ttk.pte.hu (L. Kollár).

0040-4020/$ – see front matter © 2013 Published by Elsevier Ltd.
http://dx.doi.org/10.1016/j.tet.2013.07.044

may create a more rigid, pre-organized, electron-rich binding pocket.

2. Results and discussion

Tetraiodocavitand (**1**), bearing four excellent leaving groups, was synthesized in four consecutive steps according to our well-established protocol.[5] Trimethylsilyl-ethynyl functionalities were placed on the upper rim of the cavitand scaffold under typical Sonogashira-coupling conditions (**2**, Scheme 1.). Deprotection of **2** with TBAF·3H_2O in tetrahydrofuran afforded the corresponding tetra(ethynyl)cavitand (**3**) that was subsequently used as a coupling partner in fourfold CuAAC reactions. In this study, the commercially available azidobenzene, 1-azido-4-iodobenzene, benzyl azide, poly(ethylene glycol) methyl ether azide (PEG average M_n 1000) and (*R*)-2-(azidomethyl)-1-Boc-pyrrolidine were used in the click coupling procedure in the presence of CuI at rt. In all cases, the ^1H NMR resonance corresponding to the terminal alkyne (3.01 ppm) was completely lost and replaced by the resonances of the aromatic protons of the triazole rings in the range of 7.70–9.14 ppm. All derivatives were fully characterized by IR, ^1H and ^{13}C NMR as well as by MS techniques (see Experimental section). The GPC characterization of **7** revealed an average molecular weight of M_n=5800 along with a narrow polydispersity (1.11), and the average number of repeat units was calculated to be *n*=25. Both the GPC and NMR analysis confirmed the quantitative coupling between cavitand **3** and the linear PEG chains. It is important to note that all reactions afforded the expected cavitand-based conjugates in good yields (58–82%), and in the course of this multistep synthesis starting from the condensation reaction of 2-methylresorcinol and acetaldehyde, no time-consuming chromatography was needed. Simple trituration of the products with MeOH usually afforded sufficiently pure materials. The developed procedure allowed us to extend significantly the inner cavity of these cavitands, and furthermore, incorporate various functionalities, such as additional aromatic walls (**4**, **5**, **6**), long PEG chains (**7**) and stereogenic centres (**8**). This study proved very well the high versatility and functional group tolerance of the CuAAC reaction on our macrocyclic platform. Moreover, it was expected that the addition of PEG side chains to the cavitand core could cause a change in its solubility in water. Indeed, unlike the other novel cavitand derivatives, the PEGylated cavitand (**7**) exhibited enhanced solubility in water (>25 mg mL^{-1}). On the other hand, the synthesis of a cavitand–aryl iodide conjugate (**5**) offers promise for further extension of this cavitand skeleton.

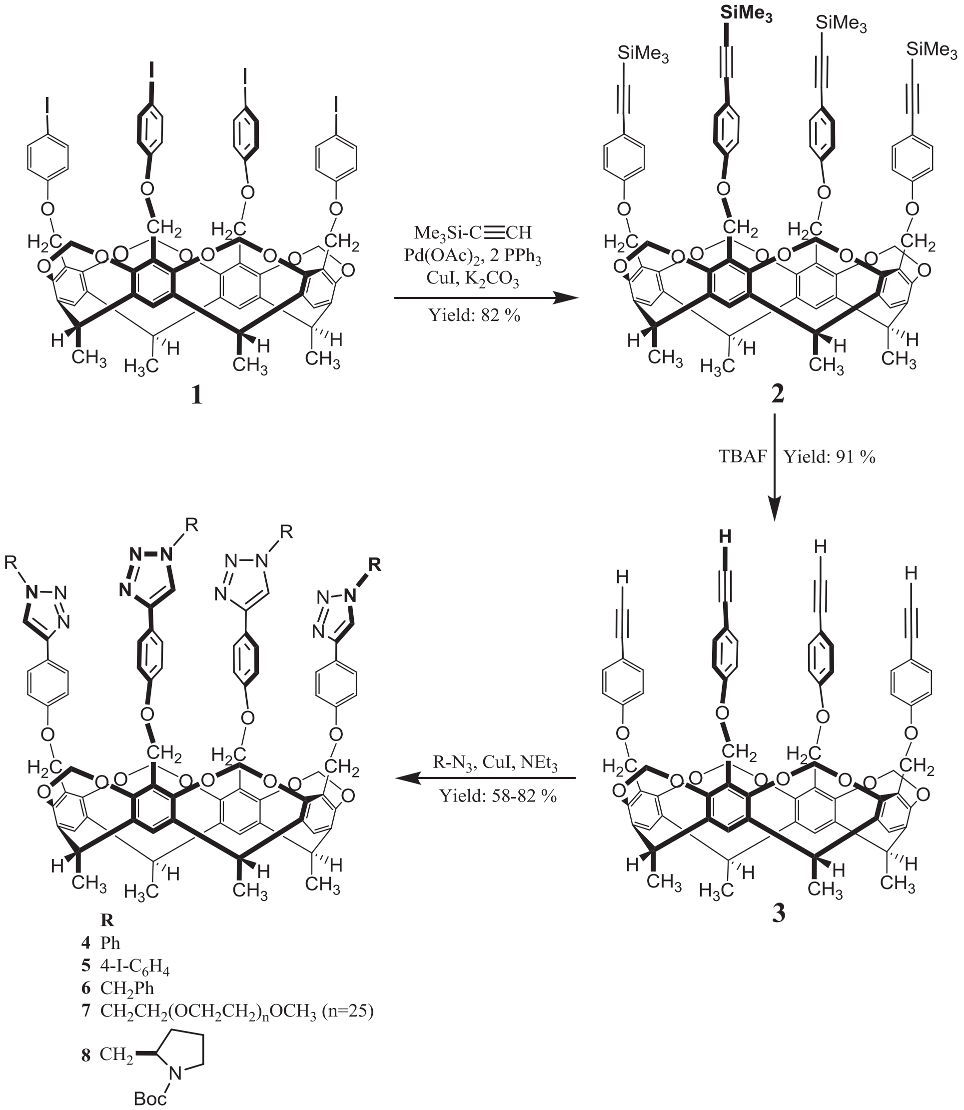

Scheme 1. Synthetic route to the novel click-based cavitands (**4**–**8**).

To the best of our knowledge, the largest covalently linked supramolecular systems containing *multiple* cavitand subunits feature molecular dimensions of 10 Å×25 Å[21,22] or an internal volume of up to 1050 Å^3 for the so-called superbowls.[23,24] Self-assembled capsules through metal–ligand interactions, and mainly, hydrogen bonding also plays a crucial part in constructing large molecular containers with internal cavities of similar volumes.[24–29] All our efforts to obtain crystals suitable for X-ray analysis were unsuccessful. However, the dimensions of cavitand **4** were found to be 9 Å×18 Å by using a semiempirical RM1 method,[30] which place it amongst the largest *unimolecular* hosts obtained by pure covalent synthesis. The energy-minimized structure of cavitand **4** is shown in Fig. 1. The angles between the neighbouring rings are approximately 90°, while the dihedral angles between the vertically positioned rings *B*/*C* and *C*/*D* vary in the range of 30.7–32.8° and 160.0–165.4°, respectively.

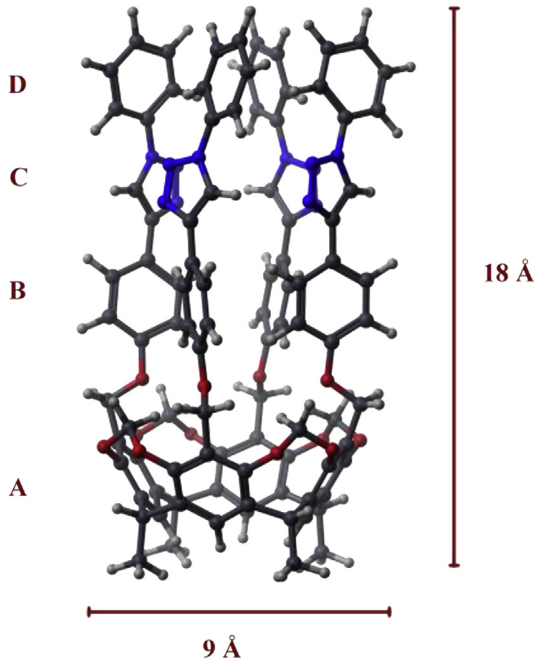

Fig. 1. The energy-minimized structure of cavitand **4**.

A DMF/water solvent mixture was used to screen the fluorescence responses of cavitand **4** upon the addition of large excess of metal ions, according to literature procedures (Fig. 2).[15–17] A similar, but less effective, quenching ability of cavitand **6** towards Cu^{2+} and Fe^{3+} was observed, therefore, all further investigations were focused on compound **4**. It should be noted that in pure DMF, the required salt concentrations could only be reached for La^{3+}, Co^{2+}, Cr^{3+}, Cu^{2+} and Fe^{3+}. A DMF/HCl solvent system was used for Zn^{2+} and Fe^{3+} in order to avoid hydrolysis in aquatic solutions. Cavitand **4** provided significant quenching in emission intensity in the presence of Cu^{2+} and Fe^{3+}. The titration profiles of cavitand **4** for the addition of Cu^{2+} and Fe^{3+} in DMF are shown in Figs. 3 and 4, respectively. When the concentration of Cu^{2+} was increased to 2000 μM, a complete fluorescence quenching was observed. Similarly, a significant decrease in fluorescent intensity occurred, when the concentration of Fe^{3+} was enhanced up to 400 μM. The binding constants of the complex formation of cavitand **4** with Cu^{2+} and Fe^{3+} were evaluated by using *Hyperquad 2006*[31] assuming 1:1 stoichiometry at various temperatures. The thermodynamic parameters were obtained according to van't Hoff theory (Fig. 5). The results indicated that the cavitand **4**–Fe^{3+} complex has higher binding constant by one order of magnitude than that of cavitand **4**–Cu^{2+}. The thermodynamic studies suggested that the complex formations of cavitand **4** with both Cu^{2+} and Fe^{3+} are mainly entropy-driven processes (Table 1).

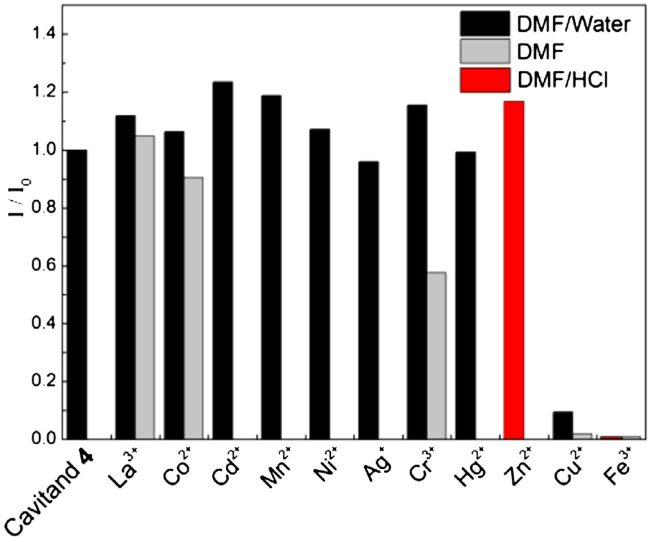

Fig. 2. Changes in fluorescence emission intensities of cavitand **4** (9.0 μM) in the presence of various metal ions (1000 μM) in various solvents. Black bar, DMF/water (90%/10%, vol/vol); red bar: DMF/0.01 M HCl (aq) (90%/10%, vol/vol); grey bar: pure DMF.

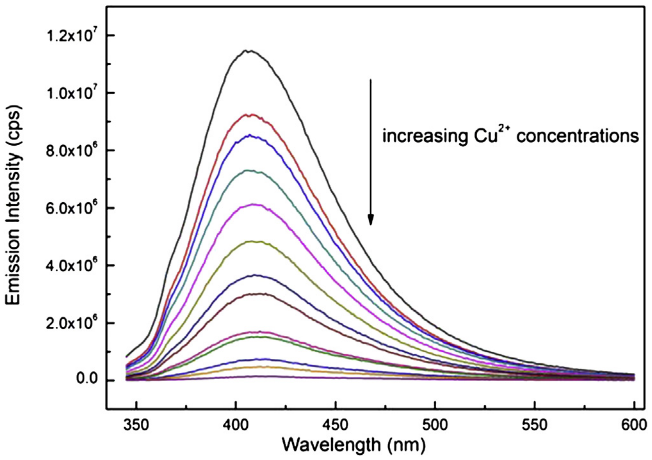

Fig. 3. Fluorescence emission response of cavitand **4** (50 μM) in pure DMF at 25 °C upon increasing concentrations of Cu^{2+} (0 μM, 200 μM, 250 μM, 300 μM, 400 μM, 500 μM, 600 μM, 750 μM, 900 μM, 1000 μM, 1250 μM, 1500 μM, 2000 μM).

3. Conclusion

Multi-level extended cavitands were synthesized in palladium-catalyzed Sonogashira-reaction followed by copper-catalyzed azide–alkyne 3+2 cycloaddition reactions. The excellent selectivities and yields make these reactions a powerful synthetic methodology for the functionalization of deepened cavitands. These cavitand hosts feature significantly enlarged molecular dimensions of at least 9 Å×18 Å. All of these cavitands, possessing highly different groups on the 'upper level' (upper portal), might serve as flexible binding pockets in 'host–guest' chemistry. Water-soluble analogues are being prepared in our laboratory that would considerably enhance their applicability in biological systems.

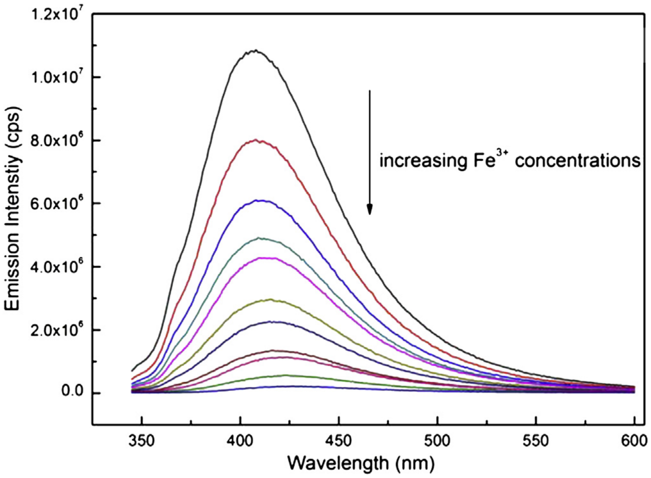

Fig. 4. Fluorescence emission response of cavitand **4** (50 μM) in pure DMF at 25 °C upon increasing concentrations of Fe^{3+} (0 μM, 40 μM, 60 μM, 80 μM, 100 μM, 125 μM, 150 μM, 200 μM, 250 μM, 300 μM, 400 μM).

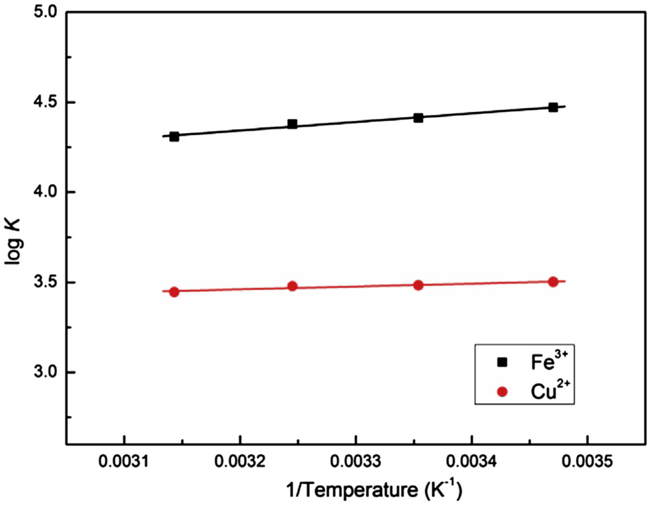

Fig. 5. van't Hoff plots for the complexations of cavitand **4**–Fe^{3+} and cavitand **4**–Cu^{2+}.

Table 1
Thermodynamic parameters for the complexations of cavitand **4**–Fe^{3+} and cavitand **4**–Cu^{2+}

	Log *K*				Δ*H*	Δ*S*
	15 °C	25 °C	35 °C	45 °C	kJ mol^{-1}	J mol^{-1} K^{-1}
Cu^{2+}	3.48(7)	3.46(8)	3.45(9)	3.41(10)	−3(1)	57(2)
Fe^{3+}	4.47(5)	4.41(8)	4.38(9)	4.31(10)	−9(1)	54(3)

4. Experimental

4.1. General information

Chemicals were either purchased or purified by standard techniques. Tetraiodocavitand (**1**) was prepared as previously described.[5] ^1H and ^{13}C NMR spectra were recorded at 25 °C in $CDCl_3$ (or in DMSO-d_6) on a 400 MHz spectrometer. The ^1H chemical shifts (δ), reported in parts per million (ppm) downfield, are referenced to the residual protons (7.26 ppm for $CDCl_3$ and 2.50 for DMSO-d_6). The ^{13}C chemical shifts are referenced to the carbon resonance of $CDCl_3$ (77.00 ppm) or to that of DMSO-d_6 (39.52 ppm), respectively.

4.2. Synthesis and characterization of cavitands 2–8

Cavitand **2**: Cavitand **1** (1.00 g, 0.658 mmol), $Pd(OAc)_2$ (16.5 mg, 0.073 mmol), PPh_3 (40 mg, 0.153 mmol) and CuI (135 mg, 0.709 mmol) were weighed, placed under an inert atmosphere into a Schlenk-tube, and deoxygenated THF (35 mL) was added. Trimethylsilylacetylene (1.1 mL, 7.784 mmol), K_2CO_3 (1.10 g, 7.959 mmol) dissolved in deoxygenated water (15 mL) was added to the reaction mixture, and then stirred at 65 °C for 16 h. The reaction mixture was partitioned between CH_2Cl_2 (50 mL) and water (50 mL). The organic phase was separated, and the aqueous phase was extracted with another portion of CH_2Cl_2 (20 mL). The combined organic phases were washed with water (50 mL), dried over $MgSO_4$ and evaporated to dryness. The residue was treated with MeOH (5 mL), the resulting precipitate was collected by filtration, and dried in vacuo. Off-white solid (760 mg, 82%), mp 184–185 °C. Anal. Calcd for $C_{84}H_{88}O_{12}Si_4$: C, 71.96; H, 6.33. Found: C, 72.25; H, 6.41. ν_{max} (KBr): 843, 868, 976, 1248, 1506, 1604, 2157 cm^{-1}; δ_H (400.13 MHz, $CDCl_3$): 0.25 (36H, s, $Si(CH_3)_3$), 1.82 (12H, d, *J* 7.2 Hz, CH_3CH), 4.61 (4H, d, *J* 7.2 Hz, inner of OCH_2O), 4.90 (8H, s, $ArCH_2O$), 5.08 (4H, q, *J* 7.2 Hz, CH_3CH), 5.74 (4H, d, *J* 7.2 Hz, outer of OCH_2O), 6.81 (8H, d, *J* 11.8 Hz, Ar), 7.37 (4H, s, Ar), 7.39 (8H, d, *J* 11.8 Hz, Ar). δ_c (100.6 MHz, $CDCl_3$): 0.1 ($Si(CH_3)_3$), 16.2 (CH_3CH), 31.2 (CH_3CH), 60.6 ($ArCH_2O$), 92.8 ($C{\equiv}C{-}SiR_3$), 100.0 (OCH_2O), 105.0 ($Ar{-}C{\equiv}C$), 114.3, 115.9, 120.7, 122.4, 133.6, 139.0, 154.0, 158.7. MS: 1424.43 $[M+23]^+$.

Cavitand **3**: To the THF (30 mL) solution of cavitand **2** (760 mg, 0.542 mmol) was added TBAF·$3H_2O$ (1.35 g, 4.279 mmol), and the reaction mixture was stirred for 30 min at rt. The solvent was evaporated, the residue was dissolved in CH_2Cl_2 (30 mL), and washed with 10% HCl (30 mL). The organic phase was dried over $MgSO_4$, and the solvent was removed on a rotary evaporator. The residue was treated with MeOH (10 mL), the resulting precipitate was collected by filtration, and dried in vacuo. Greenish-grey solid (550 mg, 91%), mp>350 °C (dec). Anal. Calcd for $C_{72}H_{56}O_{12}$: C, 77.78; H, 5.07. Found: C, 77.98; H, 5.15. ν_{max} (KBr): 974, 1246, 1506, 1604, 2106, 3286 cm^{-1}; δ_H (400.13 MHz, $CDCl_3$): 1.83 (12H, d, *J* 7.2 Hz, CH_3CH), 3.01 (4H, s, $C{\equiv}CH$), 4.63 (4H, d, *J* 7.2 Hz, inner of OCH_2O), 4.92 (8H, s, $ArCH_2O$), 5.09 (4H, q, *J* 7.2 Hz, CH_3CH), 5.76 (4H, d, *J* 7.2 Hz, outer of OCH_2O), 6.84 (8H, d, *J* 8.8 Hz, Ar), 7.39–7.43 (12H, m, Ar), δ_c (100.6 MHz, $CDCl_3$): 16.1 (CH_3CH), 31.2 (CH_3CH), 60.6 ($ArCH_2O$), 76.1 ($C{\equiv}CH$), 83.3 ($ArC{\equiv}C$), 100.0 (OCH_2O), 114.4, 114.8, 120.7, 122.3, 133.7, 138.9, 153.9, 158.9. MS: 1135.37 $[M+23]^+$.

4.2.1. General synthesis for cavitands ***4–8***. Cavitand **3** (250 mg, 0.225 mmol) and CuI (13 mg, 0.068 mmol) were weighed, placed under an inert atmosphere into an Schlenk-tube, then a mixture of deoxygenated CH_2Cl_2/H_2O (8 mL/1 mL) was added. The methyl *tert*-butyl ether (for **4** and **5**) or CH_2Cl_2 (for **6**, **7** and **8**) solution of the corresponding organic azide derivative (0.9 mmol) and NEt_3 (0.31 mL, 2.25 mmol) were added, then the reaction mixture was stirred for 16 h at rt. Distilled water (5 mL) was added at the end of the reaction, the organic phase was separated, and the aqueous phase was extracted with CH_2Cl_2 (2×5 mL). The combined organic phases were washed with water (10 mL), dried over $MgSO_4$ and evaporated to dryness.

Cavitand **4**, trituration with MeOH affords off-white solid (290 mg, 81%), mp 250–255 °C. Anal. Calcd for $C_{96}H_{76}N_{12}O_{12}$: C, 72.53; H, 4.82; N, 10.57. Found: C, 72.36; H, 4.71; N, 10.39. ν_{max} (KBr): 973, 1246, 1494, 1598 cm^{-1}; δ_H (400.13 MHz, $CDCl_3$): 1.87 (12H, d, *J* 7.2 Hz, CH_3CH), 4.77 (4H, d, *J* 7.2 Hz, inner of OCH_2O), 5.03 (8H, s, $ArCH_2O$), 5.14 (4H, q, *J* 7.2 Hz, CH_3CH), 5.82 (4H, d, *J* 7.2 Hz, outer of $\mathrm{OC}H_2\mathrm{O}$), 7.00 (8H, d, *J* 8.0 Hz, Ar), 7.40–7.55 (16H, m, Ar), 7.75–7.90 (16H, m, Ar), 8.27 (4H, s, C=C*H*), δ_C (100.6 MHz, $\mathrm{CDCl_3}$): 16.2 ($C\mathrm{H_3CH}$), 31.3 ($\mathrm{CH_3}C\mathrm{H}$), 60.6 ($\mathrm{Ar}C\mathrm{H_2O}$), 100.2 ($\mathrm{O}C\mathrm{H_2O}$), 115.0, 117.1, 120.4, 120.6, 122.8, 123.4, 127.4, 128.5, 129.6, 137.1, 138.9, 148.1, 154.1, 158.8. MS: 1611.60 [M+23]$^+$.

Cavitand **5**, trituration with MeOH and reprecipitation from $\mathrm{CH_2Cl_2}$/MeOH affords pale yellow solid (273 mg, 58%), mp>350 °C (dec). Anal. Calcd for $\mathrm{C_{96}H_{72}I_4N_{12}O_{12}}$: C, 55.08; H, 3.47; N, 8.03. Found: C, 55.36; H, 3.51, N, 7.91. ν_max (KBr): 974, 1246, 1489, 1616 cm^{-1}; δ_H (400.13 MHz, DMSO-d_6): 1.91 (12H, d, *J* 6.8 Hz, $\mathrm{C}H_3\mathrm{CH}$), 4.56 (4H, d, *J* 7.0 Hz, inner of $\mathrm{OC}H_2\mathrm{O}$), 4.92 (12H, br s, $\mathrm{ArC}H_2\mathrm{O}$ overlapping with $\mathrm{CH_3C}H$), 5.87 (4H, d, *J* 7.0 Hz, outer of $\mathrm{OC}H_2\mathrm{O}$), 7.06 (8H, d, *J* 8.4 Hz, Ar), 7.70 (8H, d, *J* 8.4 Hz, Ar), 7.82 (8H, d, *J* 8.3 Hz, Ar), 7.93–7.97 (12H, br s, Ar), 9.13 (4H, br s, C=C*H*), δ_C (100.6 MHz, DMSO-d_6): 16.1 ($C\mathrm{H_3CH}$), 31.3 ($\mathrm{CH_3}C\mathrm{H}$), 60.5 ($\mathrm{Ar}C\mathrm{H_2O}$), 94.1, 99.4 ($\mathrm{O}C\mathrm{H_2O}$), 115.1, 118.4, 121.7, 122.4, 122.7, 122.9, 126.8, 136.2, 138.5, 139.0, 147.2, 153.1, 158.5. MS: 2116.80 [M+23]$^+$.

Cavitand **6**, trituration with MeOH affords off-white solid (260 mg, 70%), mp 220–225 °C. Anal. Calcd for $\mathrm{C_{100}H_{84}N_{12}O_{12}}$: C, 72.98; H, 5.14; N, 10.21. Found: C, 73.12; H, 5.16, N, 10.14. ν_max (KBr): 972, 1245, 1497, 1615 cm^{-1}; δ_H (400.13 MHz, $\mathrm{CDCl_3}$): 1.83 (12H, d, *J* 7.2 Hz, $\mathrm{C}H_3\mathrm{CH}$), 4.69 (4H, d, *J* 7.2 Hz, inner of $\mathrm{OC}H_2\mathrm{O}$), 4.95 (8H, s, $\mathrm{ArC}H_2\mathrm{O}$), 5.09 (4H, q, *J* 7.2 Hz, $\mathrm{CH_3C}H$), 5.54 (8H, s, $\mathrm{ArC}H_2\mathrm{N}$), 5.76 (4H, d, *J* 7.2 Hz, outer of $\mathrm{OC}H_2\mathrm{O}$), 6.91 (8H, d, *J* 8.3 Hz, Ar), 7.28–7.42 (24H, m, Ar), 7.69 (8H, d, *J* 8.3 Hz, Ar), 7.75 (4H, s, C=C*H*), δ_C (100.6 MHz, $\mathrm{CDCl_3}$): 16.2 ($C\mathrm{H_3CH}$), 31.2 ($\mathrm{CH_3}C\mathrm{H}$), 54.1 ($\mathrm{Ar}C\mathrm{H_2N}$), 60.6 ($\mathrm{Ar}C\mathrm{H_2O}$), 100.2 ($\mathrm{O}C\mathrm{H_2O}$), 114.9, 119.3, 120.6, 122.7, 123.7, 127.2, 128.0, 128.6, 129.1, 134.9, 138.9, 147.9, 154.0, 158.6. MS: 1668.36 [M+23]$^+$.

Cavitand **7**, reprecipitation from $\mathrm{CH_2Cl_2}$/*n*-pentane yields brown oil that solidifies upon standing (943 mg, 82%). ν_max (KBr): 965, 1112, 1247, 1466, 2879 cm^{-1}; δ_H (400.13 MHz, $\mathrm{CDCl_3}$): 1.82 (12H, br d, *J* 7.2 Hz, $\mathrm{C}H_3\mathrm{CH}$), 3.36 (12H, s, $\mathrm{PEG{-}OC}H_3$), 3.55–3.75 (450H, br m, PEG-chain), 3.91 (8H, br s, $\mathrm{PEG{-}C}H_2\mathrm{N}$), 4.57 (8H, br s, $\mathrm{PEG{-}C}H_2\mathrm{CH_2}$), 4.69 (4H, br s, inner of $\mathrm{OC}H_2\mathrm{O}$), 4.95 (8H, s, $\mathrm{ArC}H_2\mathrm{O}$), 5.10 (4H, br q, *J* 7.2 Hz, $\mathrm{CH_3C}H$), 5.79 (4H, br s, outer of $\mathrm{OC}H_2\mathrm{O}$), 6.96 (8H, br s, Ar), 7.40 (4H, br s, Ar), 7.74 (8H, br s, Ar), 7.97 (4H, br s, C=C*H*), δ_C (100.6 MHz, $\mathrm{CDCl_3}$): 16.1 ($C\mathrm{H_3CH}$), 31.2 ($\mathrm{CH_3}C\mathrm{H}$), 50.4 ($\mathrm{PEG{-}}C\mathrm{H_2N}$), 58.9 ($\mathrm{PEG{-}O}C\mathrm{H_3}$), 60.6 ($\mathrm{Ar}C\mathrm{H_2O}$), 69.4 ($\mathrm{PEG{-}}C\mathrm{H_2CH_2}$), 70.5 (PEG-chain), 71.9 ($C\mathrm{H_2OCH_3}$), 100.1 ($\mathrm{O}C\mathrm{H_2O}$), 114.9, 120.5, 122.6, 123.5, 127.2, 138.8, 147.3, 154.0, 158.6. GPC: M_n=5800.

Cavitand **8** (isolated as a 1:1 mixture of two rotamers due to C(O)–N hindered rotation), trituration with MeOH affords light yellow solid (309 mg, 68%), mp 205–210 °C. Anal. Calcd for $\mathrm{C_{112}H_{128}N_{16}O_{20}}$: C, 66.65; H, 6.39; N, 11.10. Found: C, 66.51; H, 6.60, N, 11.01. ν_max (KBr): 975, 1247, 1499, 1616, 1693 cm^{-1}; δ_H (400.13 MHz, $\mathrm{CDCl_3}$): 1.49 (36H, s, ($\mathrm{C(C}H_3\mathrm{)_3}$)), 1.65–2.00 (28H, m, $\mathrm{C}H_3\mathrm{CH}$ overlapping with 2× pyr($\mathrm{C}H_2$)), 3.10–3.45 (12H, br m, pyr($\mathrm{C}H\mathrm{{-}N}$) overlapping with pyr($\mathrm{C}H_2\mathrm{{-}N}$)), 4.15 (4H, br s, ax. of triazole–$\mathrm{C}H_2$-pyr), 4.50–4.75 (8H, br s, eq. of triazole–$\mathrm{C}H_2$-pyr overlapping with inner of $\mathrm{OC}H_2\mathrm{O}$), 4.96 (8H, s, $\mathrm{ArC}H_2\mathrm{O}$), 5.10 (4H, q, *J* 7.2 Hz, $\mathrm{CH_3C}H$), 5.80 (4H, d, *J* 7.2 Hz, outer of $\mathrm{OC}H_2\mathrm{O}$), 6.97 (8H, d, *J* 8.0 Hz, Ar), 7.41 (4H, s, Ar), 7.70–7.80 (12H, Ar overlapping with C=C*H*), δ_C (100.6 MHz, $\mathrm{CDCl_3}$): 16.1 ($C\mathrm{H_3CH}$), 22.6 and 23.3 (pyr-$C\mathrm{H_2}$), 28.4 ($\mathrm{C(}C\mathrm{H_3)_3}$), 28.90 (pyr-$C\mathrm{H_2}$), 31.2 ($\mathrm{CH_3}C\mathrm{H}$), 46.6 and 47.0 (pyr($C\mathrm{H_2{-}N}$)), 51.5 and 52.7 (pyr($C\mathrm{H{-}N}$)), 57.1 (triazole–$C\mathrm{H_2}$-pyr), 60.6 ($\mathrm{Ar}C\mathrm{H_2O}$), 79.8 and 80.2 ($C\mathrm{(CH_3)_3}$), 100.0 ($\mathrm{O}C\mathrm{H_2O}$), 114.9, 119.9, 120.6, 122.6, 123.8, 127.1, 138.9, 147.5, 154.0, 154.7, 158.6. MS: 2018.93 [M]$^+$.

Acknowledgements

Financial support for the 'Synthesis of supramolecular systems, examination of their physicochemical properties and their utilization for separation and sensor chemistry' project (SROP-4.2.2.A-11/1/KONV-2012-0065) is gratefully acknowledged. Z.C. thanks the Bolyai Grant of the Hungarian Academy of Sciences.

Supplementary data

The details of the fluorescent measurements, the binding constant evaluation and the computational study as well as the ^{1}H and ^{13}C NMR spectra of compounds **2**–**8** are available. Supplementary data related to this article can be found at http://dx.doi.org/10.1016/j.tet.2013.07.044.

References and notes

1. Cram, D. J.; Karbach, S.; Kim, H. E.; Knobler, C. B.; Maverick, E. F.; Ericson, J. L.; Helgeson, R. C. *J. Am. Chem. Soc.* **1988**, *110*, 2229–2237.
2. Cram, D. J.; Cram, J. M. *Container Molecules and their Guests*; Royal Society of Chemistry: Cambridge, 1994.
3. *Calixarenes. A Versatile Class of Macrocyclic Compounds*; Vicens, J., Böhmer, V., Eds.; Kluwer Academic: Dordrecht, the Netherlands, 1991.
4. Csók, Z.; Kégl, T.; Párkányi, L.; Varga, Á.; Kunsági-Máté, S.; Kollár, L. *Supramol. Chem.* **2011**, *23*, 710–719.
5. Csók, Z.; Takátsy, A.; Kollár, L. *Tetrahedron* **2012**, *68*, 2657–2661.
6. Rostovtsev, V. V.; Green, L. G.; Fokin, V. V.; Sharpless, K. B. *Angew. Chem., Int. Ed.* **2002**, *41*, 2596–2599.
7. Hein, J. E.; Fokin, V. V. *Chem. Soc. Rev.* **2010**, *39*, 1302–1315.
8. Meldal, M.; Tornøe, C. W. *Chem. Rev.* **2008**, *108*, 2952–3015.
9. Mehran, N.; Bare, G. A. L.; Sherman, J. C. *Tetrahedron Lett.* **2011**, *52*, 1791–1793.
10. Hui, B. W.-Q.; Sherman, J. C. *Chem. Commun.* **2012**, 109–111.
11. Li, Y.; Giles, M. D.; Liu, S.; Laurent, B. A.; Hoskins, J. N.; Cortez, M. A.; Sreerama, S. G.; Gibb, B. C.; Grayson, S. M. *Chem. Commun.* **2011**, 9036–9038.
12. Lledó, A.; Kamioka, S.; Sather, A. C.; Rebek, J., Jr. *Angew. Chem., Int. Ed.* **2011**, *50*, 1299–1301.
13. Morales-Sanfrutos, J.; Ortega-Munoz, M.; Lopez-Jaramillo, J.; Hernandez-Mateo, F.; Santoyo-Gonzalez, F. *J. Org. Chem.* **2008**, *73*, 7768–7771.
14. Lau, Y. H.; Rutledge, P. J.; Watkinson, M.; Todd, M. H. *Chem. Soc. Rev.* **2011**, *40*, 2848–2866.
15. Chang, K.-C.; Su, I.-H.; Senthilvelan, A.; Chung, W.-S. *Org. Lett.* **2007**, *9*, 3363–3366.
16. Chang, K.-C.; Su, I.-H.; Lee, G.-H.; Chung, W.-S. *Tetrahedron Lett.* **2007**, *48*, 7274–7278.
17. Park, S. Y.; Yoon, J. H.; Hong, C. S.; Souane, R.; Kim, J. S.; Matthews, S. E.; Vicens, J. *J. Org. Chem.* **2008**, *73*, 8212–8218.
18. Tian, D.; Yan, H.; Li, H. *Supramol. Chem.* **2010**, *22*, 249–255.
19. Souchon, V.; Maisonneuve, S.; David, O.; Leray, I.; Xie, J.; Valeur, B. *Photochem. Photobiol. Sci.* **2008**, *7*, 1323–1331.
20. Jomova, K.; Valko, M. *Toxicology* **2011**, *283*, 65–87.
21. Starnes, S. D.; Rudkevich, D. M.; Rebek, J., Jr. *J. Am. Chem. Soc.* **2001**, *123*, 4659–4669.
22. Tucci, F. C.; Renslo, A. R.; Rudkevich, D. M.; Rebek, J., Jr. *Angew. Chem., Int. Ed.* **2000**, *39*, 1076–1079.
23. Barrett, E. S.; Irwin, J. L.; Edwards, A. J.; Sherburn, M. S. *J. Am. Chem. Soc.* **2004**, *126*, 16747–16749.
24. Rissanen, K. *Angew. Chem., Int. Ed.* **2005**, *44*, 3652–3654.
25. MacGillivray, L. R.; Atwood, J. L. *Nature* **1997**, *389*, 469–472.
26. Schröder, T.; Sahu, S. N.; Anselmetti, D.; Mattay, J. *Isr. J. Chem.* **2011**, *51*, 725–742.
27. Ballester, P. *Chem. Soc. Rev.* **2010**, *39*, 3810–3830.
28. Tiefenbacher, K.; Rebek, J. *J. Am. Chem. Soc.* **2012**, *134*, 2914–2917.
29. Rebek, J. *Acc. Chem. Res.* **2009**, *42*, 1660–1668.
30. Schrödinger Suite 2012 Semiempirical NDDO Module; Schrödinger LLC: New York, NY, 2012.
31. Gans, P.; Sabatini, A.; Vacca, A. *Hyperquad 2006, Version 3.1.60*; Protonic Software: Leeds, U.K., 2006.